Iranian Journal of Materials Forming 12 (1) (2025) 51-64

IJMF

Online ISSN: 2383-0042

Iranian Journal of Materials Forming

Journal Homepage: http://ijmf.shirazu.ac.ir

Research Article

Mechanical Properties and Residual Stress Measurement in the Friction Stir Welding Process of Al 6061-T6 Plates with Copper and Brass Interlayer

S. Aryanpour Kashani and M. Honarpisheh*

Faculty of Mechanical Engineering, University of Kashan, Kashan, Iran

ARTICLE INFO

Article history:

Received 29 November 2024
Reviewed 18 January 2025
Revised 3 February 2025
Accepted 1 March 2025

Keywords:

Friction stir welding
Interlayer metal
6061-T6 aluminum
Residual stress

Please cite this article as:

Aryanpour Kashani, S., & Honarpisheh, M. (2025). Mechanical properties and residual stress measurement in the friction stir welding process of Al 6061-T6 plates with copper and brass interlayer. *Iranian Journal of Materials Forming*, *12*(1), 51-64. https://doi.org/10.22099/IJMF.2025.51807.1310

ABSTRACT

Friction stir welding was used to join 6061-T6 aluminum plates with and without the addition of commercial pure copper and brass alloy (CuZn30) interlayers. The effects of these interlayers on mechanical properties, and residual stress distribution were analyzed. Tensile and microhardness tests were conducted to evaluate mechanical performance, while residual stress was measured using the contour method. Welding was performed at rotational speeds of 900 and 1120 rpm and feed rates of 25 and 50 mm/min. Results showed a 54% increase in yield strength in the no-interlayer condition and a 35% increase with a copper-interlayer compared to the base metal. The highest hardness, 158 Vickers, was recorded in the brass-interlayer joint. Residual stress analysis revealed that stresses were tensile near the weld center and compressive in the base metal. Longitudinal residual stresses were generally higher than transverse stresses. The brass interlayer led to the highest residual stress distribution, followed by the copper interlayer, indicating the interlayer's role in increasing residual stress in friction stir welding.

1. Introduction

In many industrial applications, steels are increasingly being replaced by non-ferrous alloys, particularly aluminum alloys. While aluminum alloys production is relatively straightforward, joining these materials can present significant challenge [1]. Fusion welding of aluminum has several drawbacks, including susceptiblity to defects such as hot cracking, solidification cracking, porosity, distortion, and dross, all of which negatively impact the mechanical strength and microstructural integrity of the welded joint [2, 3]. These defects often render welds unsuitable due to porosity and microstructural inconsistencies in the fusion zone [4-6]. Additionally, the mechanical properties of welded joints often fall short of those of the

* Corresponding author
E-mail address: honarpishe@kashanu.ac.ir (M. Honarpisheh)
https://doi.org/10.22099/IJMF.2025.51807.1310

base materials, prompting the development of alternative welding techniques.

In 1991, the British Welding Institute (TWI) introduced friction stir welding (FSW), a solid-state joining process for non-ferrous metals [7, 8]. FSW has proven to be an effective method for welding materials with low melting points, such as aluminum, copper, and brass. The heat generated during the FSW process results from a combination of friction and plastic deformation. Several factors influence heat production in FSW, including welding parameters, the thermal conductivity of the workpiece, tool pin and back anvil properties, and the geometry of the welding tool [9].

Since its invention, FSW has been extensively researched and adopted across various industries, including aerospace, automotive, railway, shipbuilding, heating and cooling equipment manufacturing, and nuclear waste containers [10-12]. It has been shown that depending on the alloy grade and the ability of the FSW machine, butt joints of aluminum alloys with thickness ranging from 0.3 mm to 75 mm can be welded in a single pass [13].

The ability to bond aluminum to other metals has gained significant attention due to its potential benefits, such as weight reduction and cost savings, making it highly attractive for industrial applications [14]. However, joining dissimilar metals using FSW remains challenging due to differences in heat transfer coefficients, chemical compositions, and deformation behaviors between the base metals, leading to asymmetries in heat generation and material flow [15]. Consequently, recent studies have explored the feasibility of FSW for dissimilar metal joints. Khojasteh Nezhad et al. [16] investigated FSW of 6061-T6 aluminum sheets using a commercially pure copper interlayer. Their study examined the effect of copper on joint performance and microstructure, comparing it with joints welded without an interlayer. X-ray diffraction analysis revealed the formation of intermetallic compounds such as Al_2Cu and Al_4Cu_9, which significantly increased hardness and provided a strong metallurgical bond between Al and Cu, enhancing mechanical properties. The ultimate tensile strength of the joint with the copper interlayer was 285 MPa, achieving an efficiency of 89.1% relative to the base metal and surpassing that of the joint produced without an interlayer. Tan et al. [17] investigated the microstructure and mechanical properties of friction stir-welded joints between 5A02 aluminum and pure copper (T2) using a 2.0 mm tool offset towards the aluminum. Their results demonstrated a strong metallurgical bond with an ultimate tensile strength exceeding 210 MPa and 180° bending capability without fracture at the aluminum/copper interface. X-ray diffraction analysis revealed the formation of intermetallic compounds (Al_4Cu_9, Al_2Cu, and Al-Cu), which contributed to increased hardness in the weld nugget, surpassing that of copper. Xue et al. [18] further investigated the effect of welding parameters on friction stir welding (FSW) of 1060 aluminum and commercial pure copper (99.9%). Their study found that sound joints were produced when copper was placed on the advancing side, whereas placing aluminum on the advancing side led to defects due to difficulties in copper material transport. Additionally, tool offsets greater than 2 mm towards aluminum resulted in defect-free joint, while smaller offsets led to poor mixing and defects. Higher rotational speeds improved metallurgical bonding and tensile properties, whereas a 400 rpm rotational speed caused more defects. The optimal welding condition for bending properties was achieved at 600 mm/min welding speed with a 2 mm offset, while higher speeds negatively affected bending performance. Leon et al. [19] investigated the effect of various parameters on friction stir-welded 6061-T6 aluminum sheets. Their microstructural analysis showed that the recrystallization rates depended on temperature and strain rate, with the stir zone microstructure being significantly finer than the parent material due to higher temperatures and plastic deformation. Increasing the tool rotational speed to 1200 rpm enhanced weld strength, attributed to recovery and recrystallization. The formation of fine, equiaxed grains, and very fine precipitates contributed to superior tensile properties. The stir zone width was influenced by the heat input and cooling rate, with the largest stir zone and best mechanical properties achieved at a welding speed of 16 mm/min.

Esmaeili et al. [20] investigated the defects in dissimilar FSW of 1050 aluminum and 30CuZn brass using radiography. Their mechanical analysis showed improved joints quality with increasing offset. Radiographic inspection revealed coarse and continuous brass particles in the aluminum matrix, which were linked to defect formation, including kissing bonds and voids. Although not directly visible in radiographic images, these particles served as indicators of hidden internal defects, aiding in the prevention of weld failures. Zhang et al. [21] conducted residual stress measurement of FSW6061-T6 aluminum alloy and pure copper (2T) sheets using the contour method. A 0.3 mm brass wire was cut perpendicular to the weld using wire electrical discharge machine (WEDM), and stress relief measurements were taken with a coordinate measuring machine (CMM) equipped with a laser scanner. Their findings showed tensile stresses in aluminum and compressive stress in copper, with the maximum tensile stress of 240 MPa near the thermomechanically affected zone of aluminum. Morishige et al. [22] compared FSW and laser-welded joints of Al alloy and AZ31 Mg alloy under different tool rotational speeds and feed rates. The FSW joints exhibited higher hardness in their stir zones than the AZ31 base alloy due to the formation of Mg-Al intermetallic compounds, but their hardness was lower than the fusion zone of the laser-welded joints. The stir zone hardness varied with FSW welding parameters, tool rotational speed, and welding speed, affecting heat input. Li et al. [23] investigated FSW of 1350 aluminum alloy and pure copper, using a pin offset technique in which the rotating pin was mostly plunged into the aluminum side. Defect-free welds were achieved at 1000 r/min rotational speed and of 80 mm/min feed rate. Unlike other studies, no intermetallic compounds were detected in their joint. Hardness distribution showed higher values on the copper side and greater hardness at the bottom of the joint. The resulting tensile strength and elongation were 152 MPa and 6.3%, respectively.

Song et al. [24] examined FSW of dissimilar aluminum alloys (5052 and 325J) under varying welding conditions, including material arrangement. At a 1000 rpm tool rotational speed, joints with 5052 on the advancing side exhibited superior properties compared to the reverse arrangement. Sound welds were obtained in all welding conditions when 325J was on the advancing side. However, when 325J was located on the retreating side at a rotational speed of 1500 rpm, subsurface defects were detected beneath the top surface in that region. Jafari et al. [25] studied the effect of rotational speed and feed rate on the mechanical properties of FSW 6061-T6 and 7075-T6 aluminum alloys. The best mechanical properties were achieved at a 31.5 mm/min feed rate and 560 rpm rotational speed, with yield strength of 103 MPa and tensile strength of 194 MPa. The highest hardness value (110 Vickers) was recorded at 50 mm/min feed rate and 710 rpm rotational speed. In a subsequent study, Jafari et al. [26] re-examined the effect of SiO_2 nanoparticles, spindle speed, and feed rate on residual stress and mechanical properties in FSW of 7075-T6 and 6061-T6 aluminum alloys. Residual stresses analysis using the contour method indicated tensile stresses at the sample center and compressive stresses near the edges. The addition of SiO_2 nanoparticles enhanced ultimate tensile strength while reducing yield strength and residual stress.

In this study, FSW of 6061-T6 aluminum alloy was performed using intermediate layers of copper and brass with varying thicknesses. The effect of parameters such as spindle speed and feed rate on mechanical properties and residual stress was analyzed. Despite extensive research on FSW of dissimilar metals, no previous studies have investigated this specific combination of 6061-T6 aluminum alloy with copper and brass interlayers, highlighting the novelty of this work.

2. Experimental Procedures

This study utilized 6061-T6 aluminum alloy as the base metal, while commercially pure copper and brass alloy (CuZn30) served as intermediate metals in friction stir welding (FSW). The chemical compositions of these materials are presented in Tables 1-3.

The dimensions of the metals used in this research

Table 1. Chemical composition of 6061-T6 aluminum

Elements	Al	Zn	Mg	Cu	Fe	Cr	Si
wt.%	97.1114	0.111	0.976	0.48	0.528	0.1101	0.563
Elements	Mn	Zr	Ti	Ni	Pb	Sb	Sn
wt.%	0.07987	0.001	0.01885	0.01	0	0.0029	0.007

Table 2. Chemical compositions of commercial pure copper

Elements	Cu	Zn	Sn	Al	Pb	Ni	Fe	Si
wt.%	99.32	0	0.266	0.183	0.1	0.017	0.046	0.014

Table 3. Chemical compositions of CuZn30 brass alloy

Elements	Cu	Zn	Pb	Fe	Al	Ni	Sn
wt.%	69-71	Remainder	max 0.05	max 0.05	max 0.02	max 0.3	max 0.1

are as follows:

- 6061-T6 aluminum alloy (base metal): 100 × 50 × 6 mm
- Pure commercial copper (interlayer metal): 100 × 6 × 0.8 mm
- Brass sheet (CuZn30) (interlayer metal): 100 × 6 × 0.5 mm
- Brass sheet (CuZn30) (interlayer metal): 100 × 6 × 1 mm

Since the copper and brass interlayer were produced through the rolling process, careful preparation was required to ensure their physical, mechanical, and dimensional integrity. Rolling can introduce residual stresses and structural heterogeneity which may negatively impact the welding process. To mitigate these issues, the interlayer plates were annealed at approximately 650 °C in a furnace, as shown in Fig. 1. Annealing plays a crucial role in restoring the material's properties, enhancing its performance, and ensuring its suitability for further processing. Following the annealing process, the oxidized surfaces of the samples were polished to completely remove any oxidation. The samples were then thoroughly cleaned with acetone to ensure contamination-free surfaces before welding.

Experimental testing is essential for evaluating the performance of various tool geometries under specific welding conditions. Key parameters such as weld strength, defect formation, and temperature distribution are analyzed to optimize the tool design [16, 27, 28]. Given that welding quality and tool wear are critical factors in selecting tool materials, this study utilized AISI H13 hot-worked steel for the FSW process tool. The tool featured a threaded cylindrical pin geometry with a flat shoulder, ensuring efficient material flow and minimal wear. The geometrical and schematic specifications of the tool are presented in Fig. 2. The experiments were conducted using the process parameters listed in Table 4.

To determine residual stress following cutting, samples were prepared for contour method analysis. Achieving precise cutting with minimal width and load while ensuring a smooth surface finish was crucial. For this purpose, electrical discharge machining (EDM) was employed using a 0.25-micron diameter brass wire at a cutting speed of 0.6 mm/min. The samples were bisected via wire EDM, ensuring a high-quality surface finish suitable for accurate coordinate measurement machine (CMM) readings (see Fig. 3 for a visual representation of the procedure).

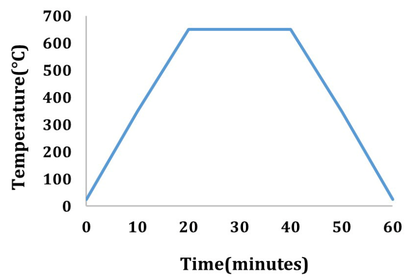

Fig. 1. Copper and brass interlayer time–temperature annealing profile.

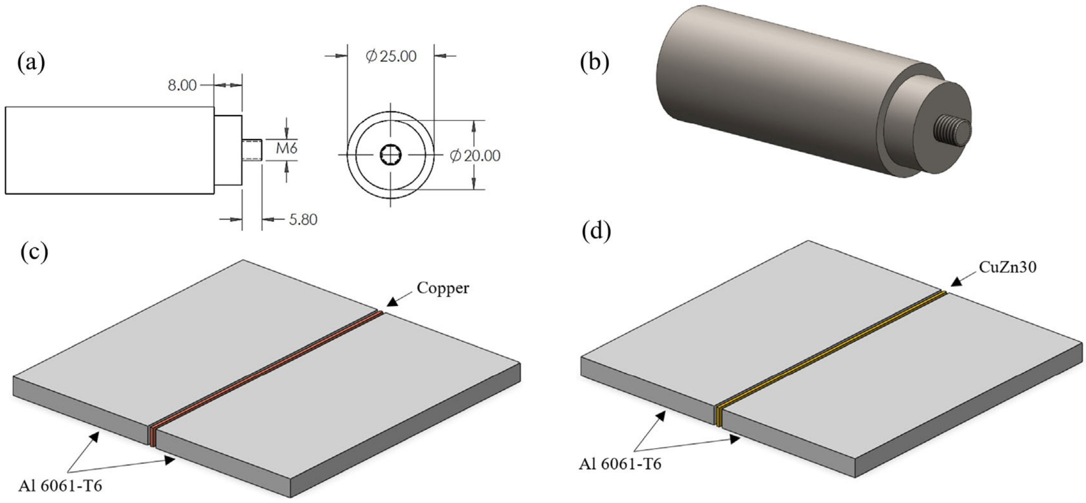

Fig. 2. (a) Tool geometry (in mm), (b) schematic of the tool used in the process, (c) positioning of aluminum and copper interlayer, and (d) positioning of aluminum and CuZn30 interlayer.

Table 4. Welding process parameters

Weld no	Interlayer (mm)	Spindle speed (rpm)	Feed rate (mm/min)
1	none	900	25
2	none	900	50
3	none	1120	25
4	none	1120	50
5	Copper (0.8)	900	25
6	Copper (0.8)	900	50
7	Copper (0.8)	1120	25
8	Copper (0.8)	1120	50
9	Brass (0.5)	900	25
10	Brass (0.5)	900	50
11	Brass (0.5)	1120	25
12	Brass (0.5)	1120	50
13	Brass (1.0)	900	25
14	Brass (1.0)	900	50
15	Brass (1.0)	1120	25
16	Brass (1.0)	1120	50

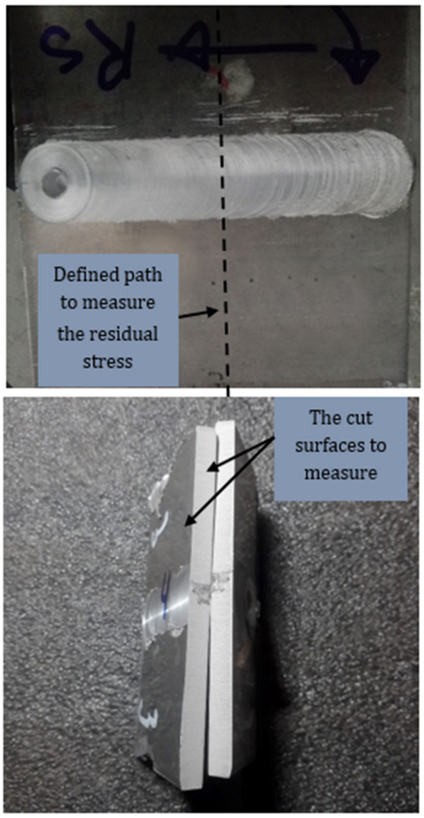

Fig. 3. Schematic of research procedure.

CMM measurements were taken across the cut surfaces, which exhibit roughness variations (peaks and valleys) in the range of 10-100 microns. Each sample had two cut surfaces analyzed. The CMM was programmed to capture data points across the entire surface with sufficient resolution to accurately map the displacement range. This resulted in two datasets per sample: one representing the nominal x and y coordinates and the other capturing the actual z deviations caused by stress release. The collected data were analyzed in MATLAB, where the actual z-values were averaged and used to generate a 3D surface plot.

A polynomial equation representing the deformation due to residual stress release was derived in MATLAB. The coefficients from this equation were then used to compute displacement values for the cut surface.

These computed displacements were applied as boundary conditions in an ABAQUS model, simulating half of the cut sample. The MATLAB-derived displacements were used to replicate the stress relaxation process, enabling accurate residual stress analysis.

Tensile test specimens were prepared in accordance with ASTM E8M standards. The tensile tests were conducted at room temperature using a Hansfield H25KS testing machine with a maximum load capacity of 25 kN. A crosshead speed of 1 mm/min was applied during the tests. In addition, the Vickers microhardness test was performed in the central region of the weld section. A static load of 100 grams was applied, with a dwell time of 10 seconds, to ensure accurate hardness measurements.

3. Results and Discussion

The weld cross-section appearance is shown in Fig. 4. For joints without an interlayer and those with a copper interlayer, the weld exhibited a flawless surface, free from cracks, holes, or grooves. However, this was not the case for a joint with a brass interlayer. A defect-free weld can be achieved by optimizing welding parameters such as tool rotation rate, welding speed, dwell time, and tool geometry. To achieve a high-quality joint, a high rotational speed combined with a low welding speed is generally required. Surface defects were observed at rotational speeds below 800 r/min and feed rates above 80 mm/min. These conditions fail to generate sufficient heat input, resulting in inadequate material flow and defect formation [28-30]. Dwell time is another critical factor in ensuring adequate heat input. However, excessively high rotational speeds can lead to excessive heat input generation, promoting grains growth and increasing intermetallic compound formation. This, in turn, negatively affects the mechanical properties of the weld [30]. Furthermore, tool vibration was identified as a challenge during the welding process. This issue can be mitigated by annealing the copper interlayer before FSW, thereby softening the material and reducing vibrations [31].

3.1. Mechanical properties

The mechanical properties of the welded joint were analyzed by evaluating the results of tensile tests, microhardness measurements, and residual stress analysis. The tensile test provided insight into key properties such as yield stress, ultimate tensile strength, and elongation percentage. The micro-hardness test was conducted to assess the hardness distribution across the cross-sectional area of the welded samples. Additionally, the contour method was employed to measure and analyze residual stress distribution in the welded joints.

The results of the tensile test for different welding conditions are shown in Fig. 5. The results obtained in this research are categorized into three main groups, allowing for a comprehensive comparison with the properties of the base metal. This categorization is presented in Table 5.

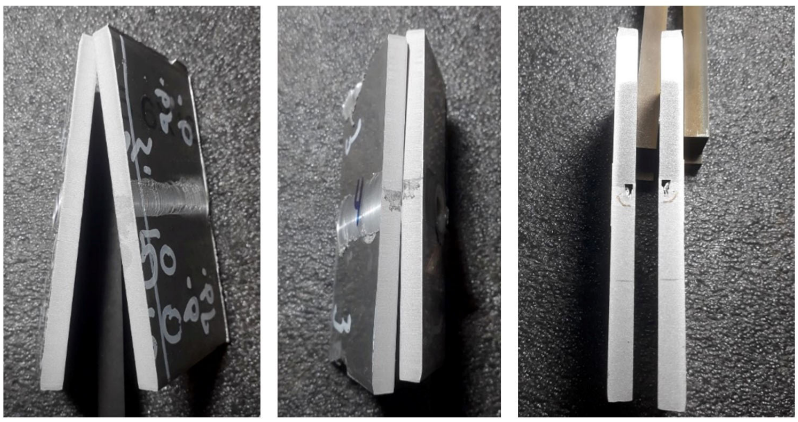

(a) (b) (c)

Fig. 4. Cross section of joints: (a) welded samples without interlayer (n = 900 rpm, f = 50 mm/min), (b) welded samples with copper interlayer (n = 900 rpm, f = 25 mm/min), and (c) welded samples with brass interlayer (n = 900 rpm, f = 50 mm/min).

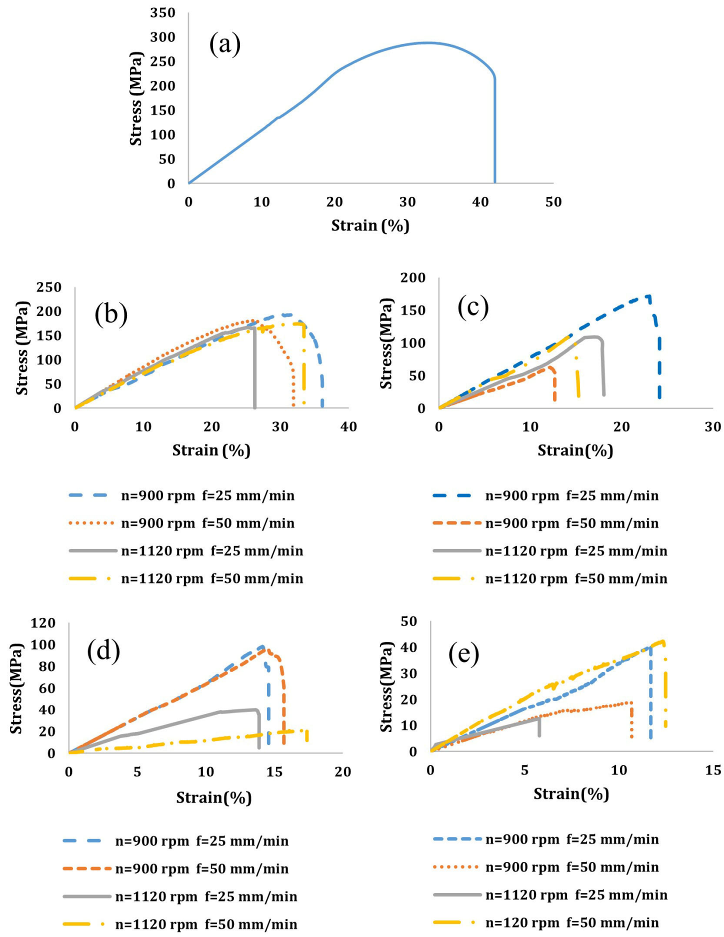

Fig. 5. Engineering stress-strain curve of: (a) aluminum plate, (b) welded samples without interlayer, (c) welded samples with copper interlayer, (d) welded samples with 0.5 mm brass interlayer, and (e) welded samples with 1 mm brass interlayer.

Table 5. Categorization of mechanical properties and comparison with base metal properties

Group	Interlayer type	Thickness (mm)
1	None	-
2	Copper	0.8
3	Brass	0.5, 1

The tensile test results indicate that the welded joints exhibit yield strength performance. The yield strength of the base material is 121 MPa. When welded without an interlayer, the yield strength increases to 185 MPa, which is 64 MPa higher than that of the base metal. With a copper interlayer, the yield strength was 163 MPa, showing an improvement of 42 MPa over the base material. However, welding with a brass interlayer resulted in a yield strength of 95 MPa, which is approximately 26 MPa lower than that of the base metal. Fig. 6 illustrates the best yield strength results across the different groups. The results of the ultimate tensile strength show a decrease in the tensile properties of the

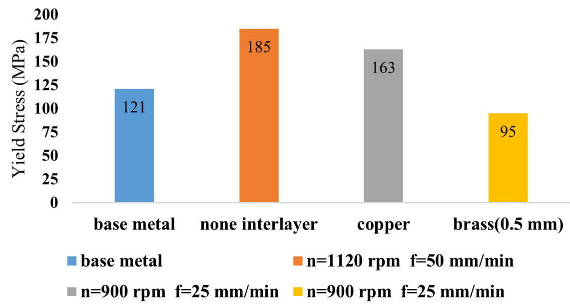

Fig. 6. Best yield strength results for different groups.

welded joints compared to the base metal. This reduction is attributed to the microstructure of the bonding zone, which has higher hardness compared to the base material, consequently lowering the tensile properties in that area. Among the tested joints, the highest tensile properties were observed in the joint without an interlayer, exhibiting a reduction of about 30% compared to the base metal. This was followed by the joint with a copper interlayer, which showed a 35%

reduction, and finally, the joint with a brass interlayer, which experienced a 65% reduction. Fig. 7 illustrates the best ultimate tensile strength results across the different groups. The results obtained from the percentage of elongation in the tensile tests indicate a decrease in the elongation of the welded joints compared to the base metal. Fig. 8 illustrates the best results for the percentage of elongation across the different groups.

The effect of the interlayer metal on the mechanical properties indicates that copper serves as a good interlayer for this process. Although its yield properties were lower than those observed with welding without an interlayer, it still provided better yield properties than the base metal. Additionally, other studies [16] have suggested that copper can yield better results compared to welding without an interlayer. On the other hand, the brass interlayer did not provide satisfactory mechanical properties in this study. This could be due to the zinc element in the brass alloy, which may not form strong mechanical properties with aluminum. Another significant factor could be the tool geometry, which, in this study, was less efficient compared to modern geometries introduced by the UK Welding Society. Additionally, welding parameters such as feed rate and

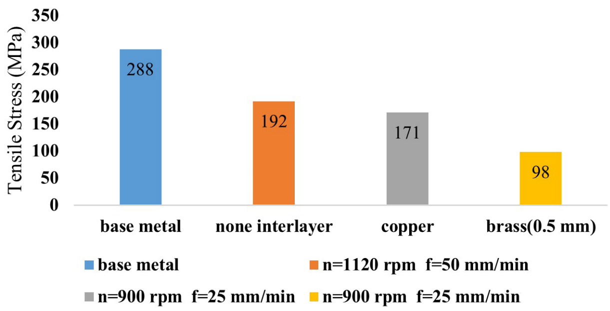

Fig. 7. Ultimate tensile strength results for different groups.

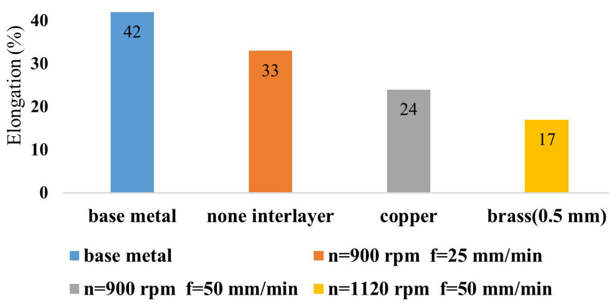

Fig. 8. Best elongation at break results for different groups.

spindle speed can significantly influence the resulting mechanical properties. The impact of spindle speed and feed rate on the results of this study is shown in Fig. 9. The results of the microhardness test for the best joints in different groups are shown in Fig. 10.

In the microhardness test, the highest measured hardness for the welded joint with a brass interlayer was approximately 160 Vickers, which is 55% higher than the hardness of the base metal. This indicates that incorporating a brass interlayer can substantially enhance the hardness of the welded joint, potentially improving its mechanical performance and durability under different conditions. For the welded joint with a copper interlayer, the highest measured was 123 Vickers, representing a 20% increase over the base metal. Notable increase in hardness when using interlayers is attributed to the formation of intermetallic compounds between copper and aluminum. These compounds, including Al_4Cu_9, Al_2Cu, and Al-Cu, have also been observed in other studies on dissimilar welds between aluminum and copper or other metals [32]. In contrast, the highest observed hardness in welding without an interlayer was 116 Vickers. The hardness variation in the welds without an interlayer was the smallest compared to the other welds. The greatest hardness variations were observed in welding with a brass interlayer, followed by welding with a copper interlayer.

3.2. Residual stress measurement ignoring interlayer effects

This section presents the results of the residual stress analysis in the weld zone with the interlayer metal effects neglected. In this study, residual stress measurements were performed on three of the best joints from different groups. The data collected from the CMM were processed and denoised using MATLAB, and the resulting 3D plots are shown in Fig. 11. In this study, considering the release of displacements along the Z-axis, the residual stress in the same direction (σ_z) is also calculated. The path of residual stress measurement along the X and Y directions in the welded samples is shown in Fig. 12.

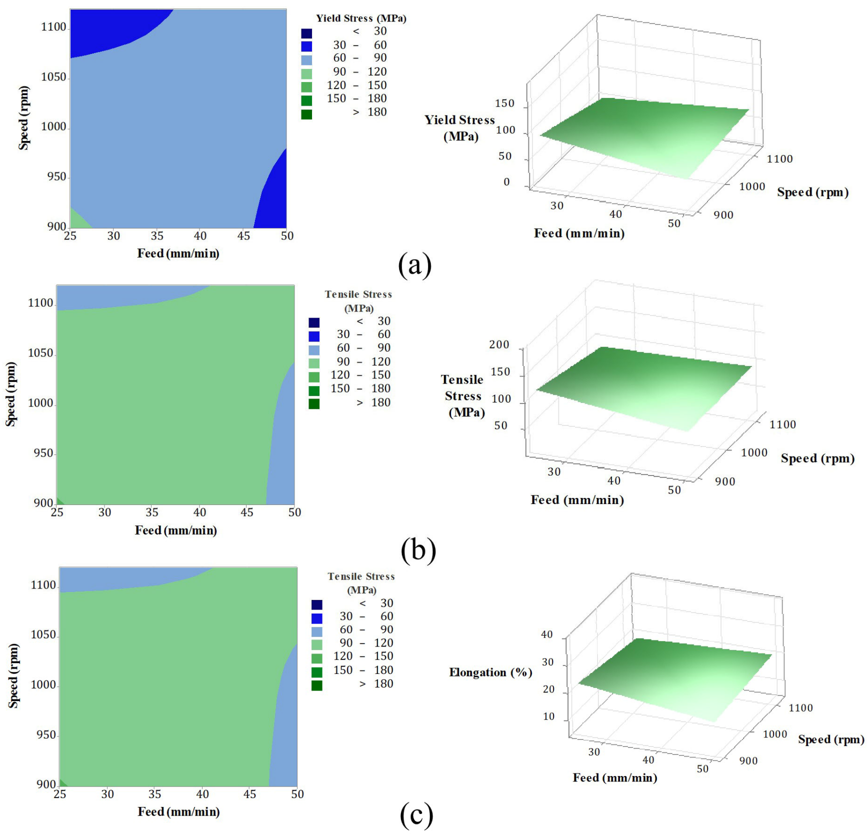

Fig. 9. Contour and surface graphs illustrating the effect of spindle speed and feed rate parameters on: (a) yield stress, (b) tensile stress, and (c) elongation.

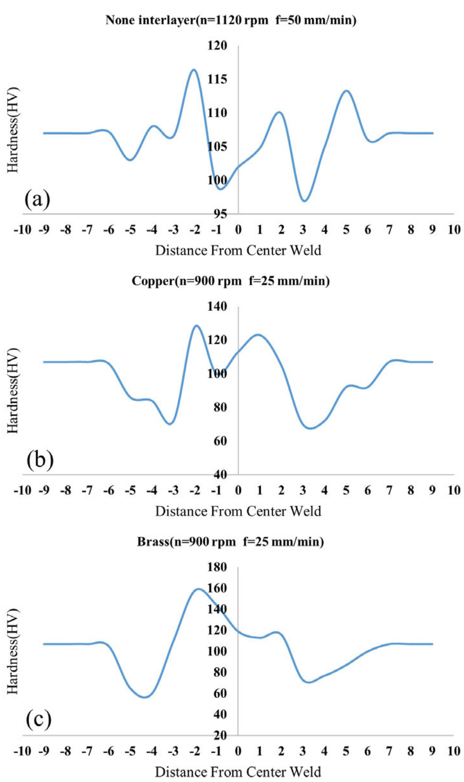

Fig. 10. Centerline hardness profile of the friction stir welded joint: (a) without interlayer, (b) with copper interlayer, and (c) with brass interlayer.

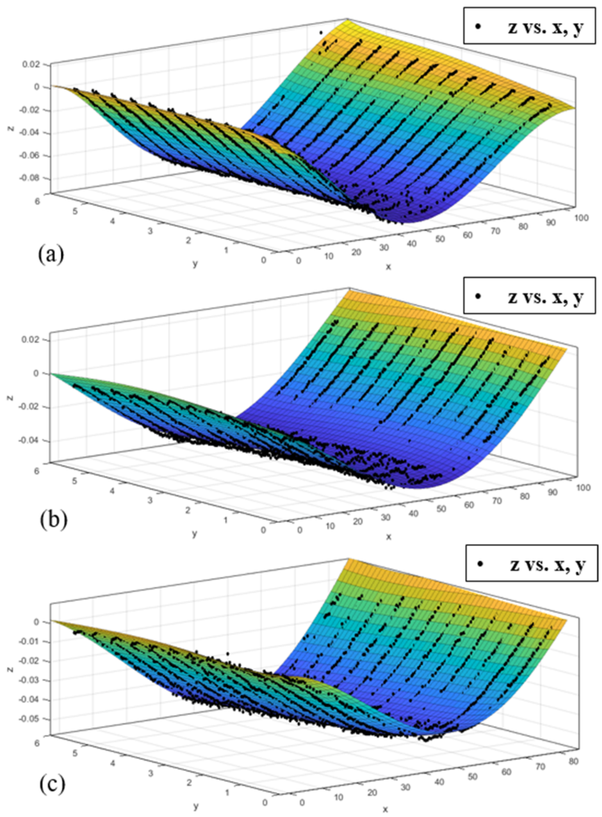

Fig. 11. 3D plot of CMM data for friction stir welding: (a) without interlayer, (b) with copper interlayer, and (c) with brass interlayer, processed in MATLAB software.

Figs. 13-15 displays the results of residual stress measurement for three different cases: without interlayer, with copper interlayer and with brass interlayer. The results obtained from the residual stress measurement in the longitudinal direction of the cross-section of the welded samples indicate that as we move closer to the center of the weld, the residual stresses transition to tensile, while on the base metal side, the residual stresses are compressive. Generally, the longitudinal residual stresses are higher than the transverse residual stresses. The distribution of residual stress in welding with a brass interlayer exhibited the highest value, followed by welding with a copper interlayer, and finally, the welding without an interlayer. This progression highlights the influence of the interlayer metal in increasing the residual stress in friction stir welding. Fig. 16 illustrates the trend of the increasing residual stress levels in the joints created.

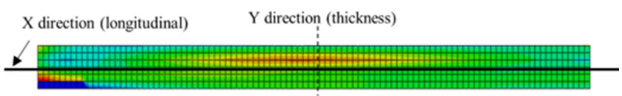

Fig. 12. Path of residual stress measurement in the X and Y directions of the welded samples.

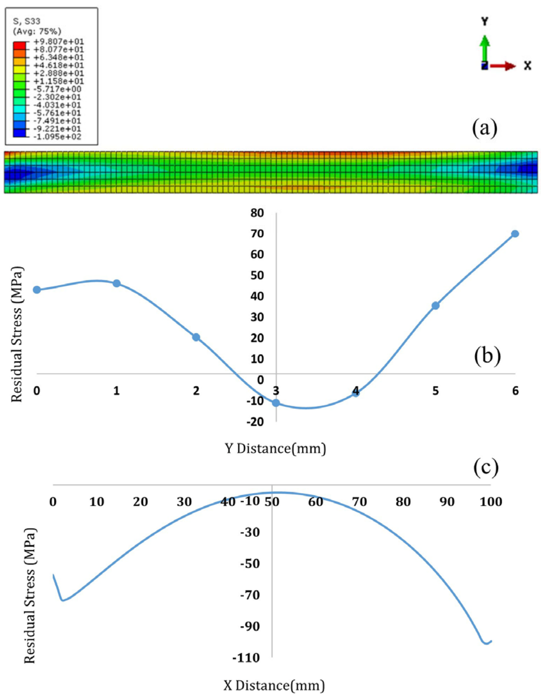

Fig. 13. Residual stress measurement results for the friction stir welded sample without an interlayer: (a) residual stress contour in the σz direction, (b) residual stress σz in the thickness direction, and (c) residual stress σz in the longitudinal direction.

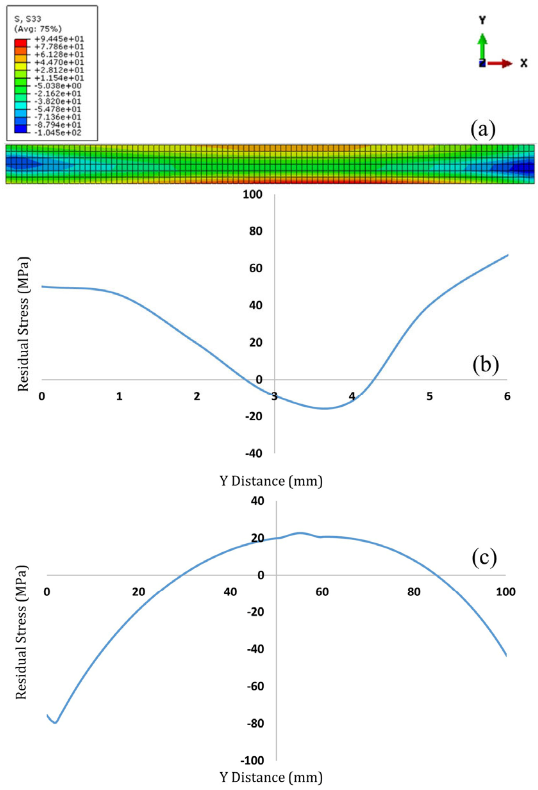

Fig. 14. Residual stress measurement results for the friction stir welded sample with copper interlayer: (a) residual stress contour in the σz direction, (b) residual stress σz in the thickness direction, (c) rtesidual stress σz in the longitudinal direction.

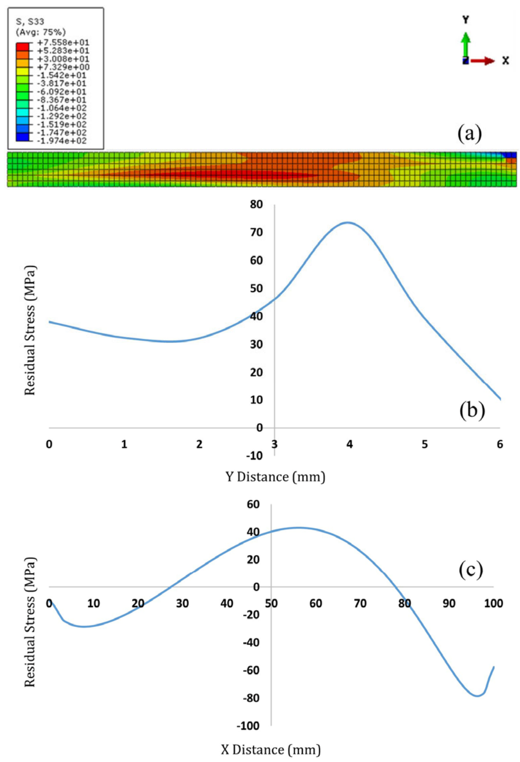

Fig. 15. Residual stress measurement results for the friction stir welded sample with brass interlayer: (a) residual stress contour in the σz direction, (b) residual stress σz in the thickness direction, and (c) residual stress σz in the longitudinal direction.

3.3. Residual stress measurement with interlayer effects

In this section, the effects of the interlayer metal on the distribution of residual stress are investigated. To achieve this, the location and precise distribution of the interlayer metal are observed using visual measurement machine (VMM) images, which are then accurately incorporated into the finite element modeling. The CMM components' data can be referenced in Fig. 11, while the results from the VMM imaging are displayed in Fig. 17.

In Fig. 18, the finite element modeling and meshing of the joining zone of the aluminum sheets are shown, with careful consideration of the interlayer particles, in ABQUS software. The results of the residual stress measurements in the samples welded with the copper and brass interlayers, considering the interlayer particles in the finite element modeling and comparing with the case without particles, are shown in Fig. 19.

The measurement path of residual stress was carried out along the Y-axis, passing through the interlayer metal particles. A comparison of the two simulations showed that the variations in residual stress were minimal or negligible. As a result, they were disregarded.

4. Conclusions

This study investigated the friction stir welding of 6T-6061 aluminum sheets in three different conditions: without an interlayer, with a copper interlayer (of 0.8 mm thick), and with a brass interlayer (0.5 mm and 1 mm thick). The experiments were conducted at rotational speeds of 900 and 1120 rpm and the feed rates of 25 and 50 mm/min. The mechanical properties of the welded joints were evaluated through tensile and microhardness tests, while residual stresses were analyzed using the contour method. The key findings are as follows:

- Sound joints were obtained in welding without an interlayer and with a copper interlayer, while welding with a brass interlayer resulted in cavity and tunnel defects.

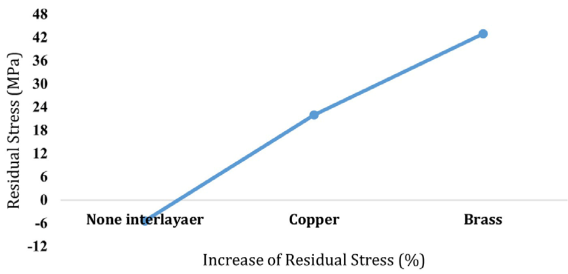

Fig. 16. Trend chart showing the increase in residual stress levels in joints without interlayer, with copper interlayer, and with brass interlayer.

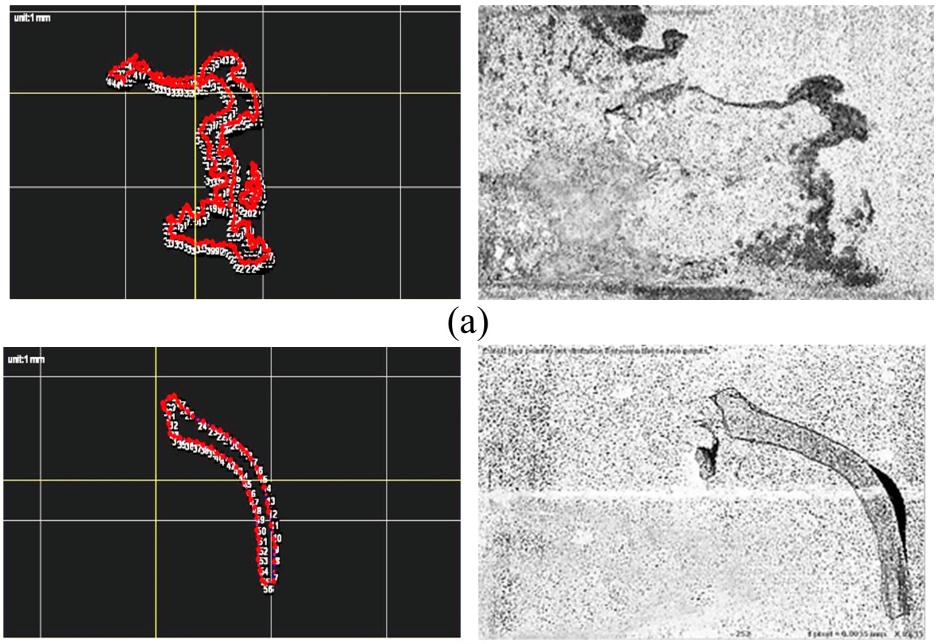

(a)

(b)

Fig. 17. VMM imaging of interlayer particles: (a) copper particles, and (b) brass particles.

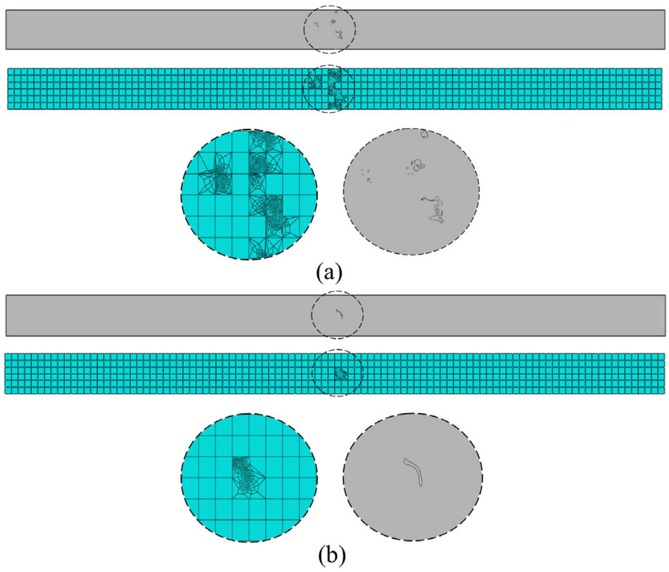

Fig. 18. Finite element modeling and meshing of the joining zone: (a) copper particles, and (b) brass particles.

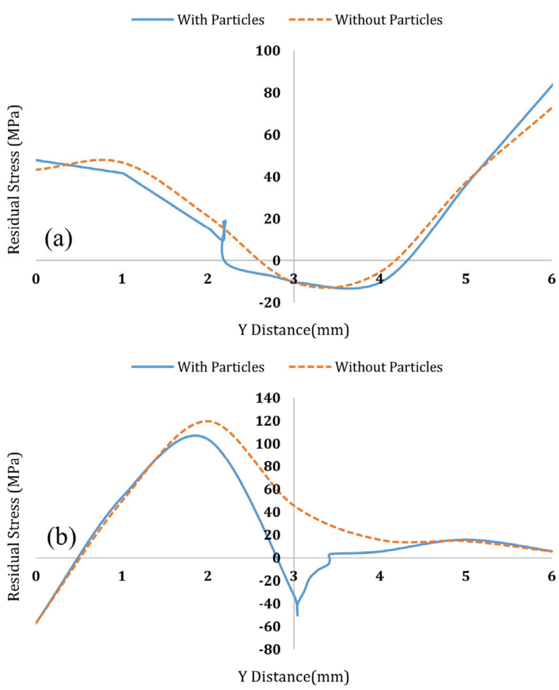

Fig. 19. Residual stress σz in the Y direction (thickness): (a) copper interlayer joint and (b) brass interlayer joint.

- Yield stress increased by approximately 54% in the joint without an interlayer, by 35% in the joint with a copper interlayer compared to the base metal, whereas welding with a brass interlayer led to a 22% decrease in yield stress.
- Ultimate tensile strength decreased by 30%, 35%, and 60% in the joints without an interlayer, with a copper interlayer, and with a brass interlayer, respectively.
- Percentage elongation decreased by 14%, 42%, and 51% in the joints without an interlayer, with a copper interlayer, and with a brass interlayer, respectively.
- The highest microhardness test was observed in the joint with a brass interlayer, showing a 55% increase compared to the base metal. The joint with a copper interlayer exhibited a 20% increase in hardness due to the formation of intermetallic compounds between aluminum and copper.
- Residual stress simulation incorporating copper and brass composite particles showed negligible differences compared to simulations without particles.
- Residual stress increased in joints with interlayers, with the highest stress observed in the brass interlayer joint, followed by the copper interlayer joint.
- In the longitudinal direction, residual stress was generally compressive in the base metal and became tensile near the joint.

Conflict of interest

The authors declare no competing interests.

Funding

No funds were received for this study.

Data Availability

The raw testing data is available upon request.

5. References

[1] Jha, A. K., Murty, S. N., Diwakar, V., & Kumar. K. S. (2003). Metallurgical analysis of cracking in weldment of propellant tank. *Engineering Failure Analysis, 10*(3), 265-273. https://doi.org/10.1016/S1350-6307(02)00073-0

[2] Doshi, S. J., Gohil, A., Mehta, N., & Vaghasiya. S. (2018). Challenges in fusion welding of Al alloy for body in white. *Materials Today: Proceedings, 5*(2), 6370-6375. https://doi.org/10.1016/j.matpr.2017.12.247

[3] Kah, P., Rajan, R., Martikainen, J., & Suoranta. R. (2015). Investigation of weld defects in friction-stir welding and fusion welding of aluminium alloys. *International Journal of Mechanical and Materials Engineering, 10*(1), 1-10. https://doi.org/10.1186/s40712-015-0053-8

[4] Ma, Z., Sharma, S., & Mishra. R. (2006). Effect of friction stir processing on the microstructure of cast A356 aluminum. *Materials Science and Engineering: A, 433*(1-2), 269-278. https://doi.org/10.1016/j.msea.2006.06.099

[5] Cao, X., Wallace, W., Immarigeon, J. P., & Poon. C. (2003). Research and progress in laser welding of wrought aluminum alloys. II. Metallurgical microstructures, defects, and mechanical properties. *Materials and Manufacturing Processes, 18*(1), 23-49. https://doi.org/10.1081/AMP-120017587

[6] Mandal, N. R. (2017). *Ship construction and welding* (Vol. 329). Springer.

[7] Rajawat, M. S., Pagrut, S., Dwivedi, S., Raj, R., & Dixit. A. R. (2022). Microstructural characterization of friction stir assisted laminated lap welding of AA6063 sheets. *Materials Today: Proceedings, 56*(949-953). https://doi.org/10.1016/j.matpr.2022.02.633

[8] Mishra, R. S., & Ma. Z. (2005). Friction stir welding and processing. *Materials Science and Engineering: R: Reports, 50*(1-2), 1-78. https://doi.org/10.1016/j.mser.2005.07.001

[9] Hossfeld, M. (2023). On friction, heat input, and material flow initiation during friction stir welding: tool and process optimization. *Journal of Manufacturing and Materials Processing, 7*(1), 34. https://doi.org/10.3390/jmmp7010034

[10] Kallee, S. W. (2010). Industrial applications of friction stir welding. In *Friction stir welding* (pp. 118-163). Woodhead Publishing.

[11] Ahmed, M. M., El-Sayed Seleman, M. M., Fydrych, D. & Çam. G. (2023). Friction stir welding of aluminum in the aerospace industry: the current progress and state-of-the-art review. *Materials, 16*(8), 2971. https://doi.org/10.3390/ma16082971

[12] Singh, V. P., Patel, S. K., Ranjan, A., & Kuriachen, B. (2020). Recent research progress in solid state friction-stir welding of aluminium–magnesium alloys: a critical review. *Journal of Materials Research and Technology, 9*(3), 6217-6256. https://doi.org/10.1016/j.jmrt.2020.01.008

[13] Sonar, T., Ivanov, M., Trofimov, E., Tingaev, A., & Suleymanova. I. (2023). A critical review on solid-state welding of high entropy alloys–processing, microstructural characteristics and mechanical properties of joints. *Defence Technology, 34*, 78-133. https://doi.org/10.1016/j.dt.2023.08.001

[14] Zhao, Y., Lu, Z., Yan, K., & Huang, L., (2015). Microstructural characterizations and mechanical properties in underwater friction stir welding of aluminum and magnesium dissimilar alloys. *Materials & Design (1980-2015), 65*, 675-681. https://doi.org/10.1016/j.matdes.2014.09.046

[15] Abd El-Hafez, H., & El-Megharbel, A. (2018). Friction stir welding of dissimilar aluminum alloys. *World Journal of Engineering and Technology*, *6*(2), 408-419. https://doi.org/10.1016/S1350-6307(02)00073-0

[16] Khojastehnezhad, V. M., & Pourasl, H. H. (2018). Microstructural characterization and mechanical properties of aluminum 6061-T6 plates welded with copper insert plate (Al/Cu/Al) using friction stir welding. *Transactions of Nonferrous Metals Society of China*, *28*(3), 415-426. https://doi.org/10.1016/S1003-6326(18)64675-8

[17] Tan, C. W., Jiang, Z. G., Li, L. Q., Chen, Y. B., & Chen, X. Y. (2013). Microstructural evolution and mechanical properties of dissimilar Al–Cu joints produced by friction stir welding. *Materials & Design*, *51*, 466-473. https://doi.org/10.1016/j.matdes.2013.04.056

[18] Xue, P., Xiao, B. L., Ni, D. R., & Ma, Z. Y. (2010). Enhanced mechanical properties of friction stir welded dissimilar Al–Cu joint by intermetallic compounds. *Materials Science and Engineering: A*, *527*(21-22), 5723-5727. https://doi.org/10.1016/j.msea.2010.05.061

[19] Leon, J. S., & Jayakumar, V. (2014). Investigation of mechanical properties of aluminium 6061 alloy friction stir welding. *International Journal of Students' Research in Technology & Management*, *2*(04), 140-144.

[20] Esmaeili, A., Givi, M. B., & Rajani. H. Z. (2012). Investigation of weld defects in dissimilar friction stir welding of aluminium to brass by radiography. *Science and Technology of Welding and Joining, 17*(7), 539-543. https://doi.org/10.1179/1362171812Y.0000000044

[21] Zhang C., & Shirzadi. A. A. (2018). Measurement of residual stresses in dissimilar friction stir-welded aluminium and copper plates using the contour method.

Science and Technology of Welding and Joining, 23(5), 394-399. https://doi.org/10.1080/13621718.2017.1402846

[22] Morishige, T., Kawaguchi, A., Tsujikawa, M., Hino, M., Hirata, T., & Higashi. K. (2008). Dissimilar welding of Al and Mg alloys by FSW. *Materials Transactions, 49*(5), 1129-1131. https://doi.org/10.2320/matertrans.MC200768

[23] Li, X. W, Zhang, D. T., Qiu, C., & Zhang, W. (2012). Microstructure and mechanical properties of dissimilar pure copper/1350 aluminum alloy butt joints by friction stir welding. *Transactions of Nonferrous Metals Society of China*, *22*(6), 1298-1306. https://doi.org/10.1016/S1003-6326(11)61318-6

[24] Song, S. W., Kim, B. C., Yoon, T. J., Kim, N. K., Kim, I. B., & Kang, C. Y. (2010). Effect of welding parameters on weld formation and mechanical properties in dissimilar Al alloy joints by FSW. *Materials Transactions*, *51*(7), 1319-1325. https://doi.org/10.2320/matertrans.M2010032

[25] Jafari, H., Honarpisheh, M., & Mansouri, H. (2019). Investigation of mechanical properties of friction stir welded dissimilar 6061-T6 and 7075-T6 aluminum alloys. In *Proceedings of the 27th Annual International Conference of Iranian Society of Mechanical Engineers (ISME2019)*. Tehran, Iran.

[26] Jafari, H., Mansouri, H., & Honarpisheh, M. (2019). Investigation of residual stress distribution of dissimilar Al-7075-T6 and Al-6061-T6 in the friction stir welding process strengthened with SiO2 nanoparticles. *Journal of Manufacturing Processes*, *43*, 145-153. https://doi.org/10.1016/j.jmapro.2019.05.023

[27] Abdollah-Zadeh, A., Saeid, T., & Sazgari. B. (2008). Microstructural and mechanical properties of friction stir welded aluminum/copper lap joints. *Journal of Alloys and Compounds, 460*(1-2), 535-538. https://doi.org/10.1016/j.jallcom.2007.06.009

[28] Akinlabi, E. T. (2010). *Characterisation of dissimilar friction stir welds between 5754 aluminium alloy and C11000 copper* [Doctoral dissertation, Nelson Mandela Metropolitan University]. http://hdl.handle.net/10948/1536

[29] Liu, P., Shi, Q., Wang, W., Wang, X., & Zhang, Z. (2008). Microstructure and XRD analysis of FSW joints for copper T2/aluminium 5A06 dissimilar materials. *Materials Letters*, *62*(25), 4106-4108. https://doi.org/10.1016/j.matlet.2008.06.004

[30] Bisadi, H., Tavakoli, A., Sangsaraki, M. T., & Sangsaraki, K. T. (2013). The influences of rotational and welding speeds on microstructures and mechanical properties of friction stir welded Al5083 and commercially pure copper sheets lap joints. *Materials & Design*, *43*, 80-88. https://doi.org/10.1016/j.matdes.2012.06.029

[31] Zhang, Q. Z., & Wei, L. I. U. (2015). Microstructure and mechanical properties of dissimilar Al–Cu joints by friction stir welding. *Transactions of Nonferrous Metals Society of China*, *25*(6), 1779-1786. https://doi.org/10.1016/S1003-6326(15)63783-9

[32] Xue, P., Ni, D. R., Wang, D., Xiao, B. L., & Ma, Z. Y. (2011). Effect of friction stir welding parameters on the microstructure and mechanical properties of the dissimilar Al–Cu joints. *Materials Science and Engineering: A*, *528*(13-14), 4683-4689. https://doi.org/10.1016/j.msea.2011.02.067